

Strong Gravity Effects of Rotating Black Holes: Quasiperiodic Oscillations

Alikram N. Aliev

*Yeni Yüzyıl University, Faculty of Engineering and Architecture,
Cevizlibağ-Topkapı, 34010 Istanbul, Turkey*

Göksel Daylan Esmer

Istanbul University, Department of Physics, Vezneciler, 34134 Istanbul, Turkey

Pamir Talazan

TÜBİTAK-BİLGEM, 41470 Gebze, Kocaeli, Turkey

(Dated: February 5, 2013)

Abstract

We explore strong gravity effects of the geodesic motion in the spacetime of rotating black holes in general relativity and braneworld gravity. We focus on the description of the motion in terms of three fundamental frequencies: The *orbital* frequency, the *radial* and *vertical* epicyclic frequencies. For a Kerr black hole, we perform a detailed numerical analysis of these frequencies at the innermost stable circular orbits and beyond them as well as at the characteristic stable orbits, at which the radial epicyclic frequency attains its highest value. We find that the values of the epicyclic frequencies for a class of stable orbits exhibit good qualitative agreement with the observed frequencies of the twin peaks quasiperiodic oscillations (QPOs) in some black hole binaries. We also find that at the characteristic stable circular orbits, where the radial (or the vertical) epicyclic frequency has maxima, the vertical and radial epicyclic frequencies exhibit an approximate 2 : 1 ratio even in the case of near-extreme rotation of the black hole. Next, we perform a similar analysis of the fundamental frequencies for a rotating braneworld black hole and argue that the existence of such a black hole with a negative tidal charge, whose angular momentum exceeds the Kerr bound in general relativity, does not confront with the observations of high frequency QPOs.

I. INTRODUCTION

Black holes are one of the most exciting objects of study in modern theoretical physics and astrophysics. They occupy a central place in all theories of gravity formulated in various spacetime dimensions.

A. Black holes in general relativity and braneworld gravity

In four dimensions, general relativity (GR) admits a family of stationary black hole solutions which turns out to be crucial for understanding its nature and the occurrence of spacetime singularities [1]. These solutions possess a number of striking properties such as uniqueness and stability, hidden symmetries and integrability of geodesics etc. [2–4] (see also [5, 6]). Altogether, these properties pave the way for astrophysical implications of GR in the regime of strong gravity, stimulating the search for black holes in the physical universe.

An astrophysical black hole is thought to be described by an exact solution of GR, discovered by Kerr [7]. This solution is uniquely characterized by two parameters: The mass and the angular momentum. In [4], it was first shown that the Hamilton-Jacobi equation for geodesics in the Kerr metric admits a complete separation of variables that is, the geodesic motion is completely integrable in this spacetime. In subsequent developments, various aspects of the geodesic motion in the Kerr metric have been extensively explored by many authors (for instance, see [5] and references therein). Among these results, the calculations of the observable orbits of test particles are of particular interest. The authors of [8] were the first to give a complete description of these orbits for the circular motion in the equatorial plane of the Kerr black hole. In particular, they found that for an extreme rotating Kerr black hole, the binding energy of the innermost stable circular orbit (ISCO) (the maximum amount of energy released by a particle approaching this orbit) can attain nearly 42% of the particle rest-mass energy, whereas for a Schwarzschild black hole it is about 6%. The high efficiency of this process led to the idea of invoking an accretion disk around a black hole to explain enormous energy output from both X-ray binaries and active galactic nuclei (for details, see [9]).

In higher dimensions, there exist a number of important black hole solutions with unexpected physical characteristics, such as dynamical instability, different horizon topologies

and different rotation dynamics. Among them, the most interesting black hole solution is given by the Myers-Perry metric [10], which is supposed to be a generalization of the Kerr solution to all number of spacetime dimensions. However, this solution is not unique, unlike the Kerr solution. In five-dimensional vacuum gravity there exists a rotating *black ring* solution [11], which may have the same mass and angular momentum as the Myers-Perry solution.

On the other hand, the higher-dimensional black holes may have observable consequences as well. We recall that some phenomenological aspects of *string/M* theory lead to braneworld scenarios, which imply that our physical universe is geometrically described by a (3+1)-dimensional hypersurface (a “3-brane”) embedded in higher dimensions [12, 13]. A complete description of black holes in such scenarios is a thorny issue and many aspects of it still remain open. Remarkably, there are several simplifying approaches which provide an intriguing description. For instance, if the size of the black hole is much smaller than the scale of the extra dimensions, the black hole would behave as a higher-dimensional object. To good enough approximation, one can argue that these black holes are described by Myers-Perry type solutions of the Einstein field equations in higher dimensions. Furthermore, the fact that in the braneworld scenarios the scale of quantum gravity becomes as lower as TeV-energy scales indicates that the small-size black holes would have been detected at high energy experiments [14, 15]. Of course, there always exists the question of gravitational stability of the Myers-Perry type black holes on the brane, whose final status is still not clear. Some interesting aspects of this issue were investigated in [16].

As for the large black holes, for which the size of the horizon is much larger than the length scale of the extra dimensions, they would also carry the imprints of the extra dimensions though “effectively” they must look like four-dimensional objects. In one approach employed in [17], it was suggested that such a black hole in the Randall and Sundrum (RS) braneworld scenario could be described by the ordinary Schwarzschild solution on the brane, which in five dimensions would look like a *black string*. The main drawback here is that the black string solution suffers from curvature singularities, propagating along the extra dimension. This solution also suffers from classical Gregory-Laflamme instabilities [18]. In another approach, such black holes were described by postulating the metric form and solving the effective gravitational equations on the RS brane [19, 20]. This idea is also reinforced by the fact that in the low energy limit, the RS braneworld scenario supports the properties of

four-dimensional GR on the brane [21, 22]. It is interesting that in this approach one can analytically describe, to some extent, the braneworld black holes by a Reissner-Nordstrom type solution in the static case [19] and by a Kerr-Newman type solution in the rotating case [20]. The tidal charge appearing in both solutions and being the imprint of the extra fifth dimension supersedes the square of the electric charge in the usual Reissner-Nordstrom and Kerr-Newman solutions. Furthermore, the tidal charge in these solutions may have both *positive* and *negative* values. On a par with the Kerr black hole, the rotating braneworld black hole can be considered as the useful and the simplest model to explore the physical effects of the tidal charge, though the gravitational stability of the latter remains an open problem. Some astrophysical implications of the braneworld black holes have recently been discussed in [23–26].

B. High-frequency quasiperiodic oscillations

Nowadays, astronomical observations provide compelling evidence for the existence of black holes in the universe. To focus only on black holes in X-ray binaries, today 23 black holes are known and 32 X-ray binaries are thought to contain black hole candidates [27]. Observations of the X-ray binaries with both black holes and black hole candidates have revealed finite-width peaks in the X-ray spectra, which can be thought of as signatures of high-frequency (> 40 Hz) *quasiperiodic oscillations* (QPOs) of the black hole accretion disk. Furthermore, in a number of sources, two peaks of QPOs have been detected. The associated frequencies of these peaks are (300, 450 Hz) for X-ray binary GRO J1655-40; (113, 168 Hz) for X-ray binary GRS 1915 + 105; (184, 276 Hz) for X-ray binary XTE J1550-564 and (165, 241 Hz) for X-ray binary H 1743-322, harboring a black hole candidate. The twin frequencies are in a 3:2 ratio. The source GRS 1915 + 105 also exhibits a pair (164, 328 Hz) which is in a 2:1 ratio (see [28] for further details).

Observations of such frequencies are certainly of fundamental importance as they may provide crucial probes of strong gravity near the black holes. Moreover, when combined with the measurements of the angular momenta of black holes [29, 30], they raise once again the old compelling question: *What is the bona fide geometry of the spacetime around the black holes?* For instance, as argued in [30], the lower bound on the angular momentum of a black hole in the X-ray binary GRS 1915 + 105 turns out to be very close to the (upper) Kerr

bound in GR. This raises the question: *Does the Kerr solution of GR describe the observed black holes with the high value of the angular momentum?* Today it remains unknown how future observational data will deal with these questions. However, this perspective in itself is very challenging for further study of observable effects of black holes in both GR and beyond it, including the cases with the violation of the Kerr bound. Some effects of rotating black holes in string theory, for which the Kerr bound is breached, were recently studied in [31].

It is also interesting that in a number of theoretical models explaining the origin of high frequency QPOs, general relativistic epicyclic frequencies of the geodesic motion have been considered as “building blocks”, though the precise mechanism still remains unknown [28, 32–34]. The successive theory of the epicyclic motion around the Kerr black holes in general relativity (with an electric charge or with an external uniform magnetic field) was developed in [35] (see also companion papers [36–38]). The authors, for the first time, obtained closed analytical expressions for the epicyclic frequencies of radial and vertical oscillations and put forward an idea of nonlinear resonances, which may occur when these frequencies are in a rational relation [35]. Afterwards, analytic expressions for the frequency of radial and vertical oscillations were also appeared in [39, 40] in the context of the analysis of trapped oscillations of an accretion disk around the Kerr black hole. The theory of epicyclic motion and the idea of nonlinear resonances have been utilized in [33, 34], even reproducing in some cases the plots of [35] for the positions of nonlinear resonances, to explain the observed frequency ratios of high frequency QPOs in black hole binaries.

C. Motivation and the basic idea

In light of all these developments, it becomes of interest to return once more to the exploration of the observable effects of a strong gravity regime encoded in the geodesic motion around rotating black holes. Our motivation for this arises from the fact that the epicyclic frequencies of the geodesic motion, as mentioned above, lie at the root of theoretical models for the observed high frequency QPOs in black hole binaries. Furthermore, the continuing success with the measurements of the angular momentum of black holes motivates us to explore the effects of the geodesic motion not only for rotating black holes in GR, where the Kerr bound on the angular momentum holds, but also for rotating black holes in a

braneworld, for which the Kerr bound may be breached. The basic idea of the present paper is as follows:

(i) To perform a detailed numerical analysis of the epicyclic frequencies at the stable circular orbits of interest in the Kerr field, using the general analytical expressions found in earlier papers [35, 36]. Thus, “monitoring” the behavior of these frequencies at the stable orbits, especially at those where the radial (or the vertical) epicyclic frequency attains its highest value, we intend to clarify the question: *Whether the simple model of pure general relativistic geodesic motion can provide observationally viable values for the epicyclic frequencies and their ratios?*

(ii) To extend the numerical analysis of the epicyclic frequencies to the case of a rotating braneworld black hole as well. The fact that the associated spacetime metric has the Kerr-Newman type form with the tidal charge (instead of the square of the electric charge) and for the negative tidal charge, the angular momentum of the black hole exceeds the Kerr bound makes this model very instructive. It is also important to note that the circular motion in this model may occur in stable orbits, unlike the case of the ordinary black holes in higher dimensions, for instance, the case of Myers-Perry black holes [41]. Exploring the behavior of the epicyclic frequencies at particular orbits of interest and comparing the results with those for the Kerr black hole we want to address the issues: *How the presence of the tidal (positive or negative) charge influences the values of the epicyclic frequencies? Does the potential existence of over-rotating braneworld black holes confront with modern observations of high frequency QPOs in black hole binaries?*

The organization of the paper is as follows: In Sec.II we begin by a brief review of the salient features of the geodesic motion in the Kerr metric and give analytic expressions for the epicyclic frequencies of radial and vertical oscillations. Next, we present the results of a detailed numerical analysis of these frequencies at the stable circular orbits of interest. In Sec.III we briefly discuss the salient properties of a rotating black hole, localized on a 3-brane in the Randall-Sundrum scenario as well as those of the geodesic motion in the field of this black hole. Here we present analytic expressions for the epicyclic frequencies of radial and vertical oscillations and perform their full numerical analysis, focusing on the stable orbits, where the radial epicyclic frequency reaches its maximum value. We also discuss the observational signature of the negative tidal charge carried by the braneworld black hole and argue that the idea that such a black hole can potentially exist in the universe does not

confront with the observations of high frequency QPOs in black holes binaries. In Sec.IV we conclude with a brief discussion of our new results.

II. GEODESIC MOTION AND EPICYCLIC FREQUENCIES IN THE SPACETIME OF KERR BLACK HOLES

We begin with the Kerr spacetime which in the Boyer-Lindquist coordinates is given by the metric

$$ds^2 = -\frac{\Delta}{\Sigma} \left(dt - a \sin^2 \theta d\phi \right)^2 + \Sigma \left(\frac{dr^2}{\Delta} + d\theta^2 \right) + \frac{\sin^2 \theta}{\Sigma} \left[a dt - (r^2 + a^2) d\phi \right]^2, \quad (1)$$

where

$$\Delta = r^2 + a^2 - 2Mr, \quad \Sigma = r^2 + a^2 \cos^2 \theta, \quad (2)$$

and M is the mass, a is the rotation parameter or the angular momentum per unit mass, $a = J/M$. The most striking feature of this spacetime is that it contains a rotating black hole. This becomes evident by the existence of the event horizon which is governed by the equation $\Delta = 0$. The largest root of this equation given by

$$r_+ = M + \sqrt{M^2 - a^2} \quad (3)$$

determines the radius of the horizon. The event horizon, as follows from this expression, exists provided that $a \leq M$. Thus, *a rotating black hole in general relativity must possess an angular momentum not exceeding its mass.*

Another remarkable feature of the Kerr spacetime is that it admits the complete separation of variables in the Hamilton-Jacobi equation for geodesics. The global time-translational and rotational symmetries of this spacetime, along with its hidden symmetries, make the Hamilton-Jacobi equation completely integrable [4] (see also [5]). For our purposes in the following, we will focus only on the motion of test particles in the equatorial plane $\theta = \pi/2$. From the symmetry considerations, it follows that such a motion will occur in circular (cyclic) orbits. Following works of [35–38], one can simply describe the circular motion and its perturbations, i.e. off-equatorial (epicyclic) motion, using the method of successive approximations in the geodesic equation

$$\frac{d^2 x^\mu}{ds^2} + \Gamma_{\alpha\beta}^\mu \frac{dx^\alpha}{ds} \frac{dx^\beta}{ds} = 0, \quad (4)$$

where the parameter s denotes the proper time along the geodesics and $\Gamma_{\alpha\beta}^{\mu}$ are the Christoffel symbols of the spacetime metric. Clearly, for the circular motion in the equatorial plane $r = r_0$, $\theta = \pi/2$, one can introduce the position vector $z^{\mu}(s) = \{t(s), r_0, \pi/2, \Omega_0 t(s)\}$, where Ω_0 is the orbital frequency. Next, using the Christoffel symbols for the Kerr metric it is easy to show that for the circular motion, the $\mu = 0, 2, 3$ components of equation (4) become trivial, whereas the remaining component with $\mu = 1$ yields

$$\Omega_0 = \frac{\pm \Omega_s}{1 \pm a\Omega_s} . \quad (5)$$

where $\Omega_s = M^{1/2}/r^{3/2}$ is the usual Kepler frequency, the upper sign refers to direct orbits (the motion of the particle and the rotation of the black hole occur in the same direction) and the lower sign refers to retrograde orbits (the motion of the particle is opposite to the rotation of the black hole). Using equation (5) in the normalization condition for the four-velocity, $g_{\mu\nu}u^{\mu}u^{\nu} = -1$, we obtain the expression for energy of the particle

$$\frac{E}{m} = \frac{r^2 - 2Mr \pm a\sqrt{Mr}}{r \left(r^2 - 3Mr \pm 2a\sqrt{Mr} \right)^{1/2}} , \quad (6)$$

where $E = mu_0$. This expression was first found and studied in [8]. The vanishing denominator of this expression, determines the radius r_{ph} of the limiting photon orbit. That is, the circular motion exists only in the region $r > r_{ph}$. It is not difficult to show that for an extreme Kerr black hole, $a = M$, we have $r_{ph} = M$ for direct orbits and $r_{ph} = 4M$ for retrograde orbits, while for $a = 0$, we find that $r_{ph} = 3M$.

To describe the epicyclic motion, we introduce a deviation vector

$$\xi^{\mu}(s) = x^{\mu}(s) - z^{\mu}(s) , \quad (7)$$

and expand equation (4) in powers of $\xi^{\mu}(s)$ about the circular orbits. Focusing on the linear approximation, it is straightforward to show that the epicyclic motion amounts to two decoupled oscillations in the radial and vertical directions (the details can be found in [35, 36] and in recent works [25, 42]). For the frequency of radial oscillations, we have

$$\Omega_r^2 = \Omega_0^2 \left(1 - \frac{6M}{r} - \frac{3a^2}{r^2} \pm 8a\Omega_s \right) , \quad (8)$$

whereas the frequency of vertical oscillations is given by

$$\Omega_{\theta}^2 = \Omega_0^2 \left(1 + \frac{3a^2}{r^2} \mp 4a\Omega_s \right) . \quad (9)$$

The stability of the circular motion against small oscillations is determined by the conditions $\Omega_r^2 \geq 0$ and $\Omega_\theta^2 \geq 0$. From the condition for the radial stability, one can infer the radii of the innermost stable circular orbits (ISCOs). As it was first shown in [8], for a nonrotating black hole, $a = 0$, we have $r_{ms} = 6M$, while for the extreme rotating case, $a = M$, we find that $r_{ms} = M$ for the direct orbit and $r_{ms} = 9M$ for the retrograde one. Meanwhile, it is easy to verify that the expression in (9) is always nonnegative in the region of existence and radial stability of the circular motion. That is, the motion is stable with respect to small oscillations in the vertical direction.

To summarize, the description of the circular motion and its small perturbations in the Kerr field inevitably results in three different fundamental frequencies, Ω_0 , Ω_r and Ω_θ , unlike the case of Newtonian gravity, where all the three frequencies turn out to be the same as the Kepler frequency, $\Omega_0 = \Omega_r = \Omega_\theta = \Omega_s$. (We note that for the Schwarzschild black hole two of these different frequencies are different. Namely, Ω_r and $\Omega_\theta = \Omega_0 = \Omega_s$). It is the regime of strong gravity near the Kerr black hole, combined with its rotational dynamics, that distinguishes between the three fundamental frequencies. Therefore, the values of these frequencies at the radii of physical interest are of great importance for astrophysical implications of the Kerr black hole.

In the following, we use the coordinate frequency ν in physical units, instead of the angular frequency $\Omega = 2\pi\nu$, as well as the characteristic frequency scale $\nu_l = c^3/2\pi GM \simeq 3.2 \cdot 10^4 (M_\odot/M) Hz$. We recall that here c is the speed of light, G is the gravitational constant and M_\odot is the mass of the Sun. With this in mind and using expression (5), we find that the orbital frequency around an extreme rotating black hole ($a = M$) is

$$\nu_0 = \frac{1}{2} \nu_l \simeq 1.6 \cdot 10^4 \left(\frac{M_\odot}{M} \right) Hz \quad (10)$$

for the direct ISCO whereas, it is given by

$$\nu_0 = \frac{1}{26} \nu_l \simeq 1.2 \cdot 10^3 \left(\frac{M_\odot}{M} \right) Hz \quad (11)$$

for the retrograde ISCO. We have performed a detailed numerical analysis of the orbital and vertical frequencies at ISCOs around a Kerr black hole with mass $M = 10M_\odot$. The results of calculations are given in Table I. We note that as the rotation parameter of the black hole grows, the radius of the direct ISCO moves towards the event horizon and the associated orbital frequency increases, approaching its maximum value in (10). The vertical

epicyclic frequency attains its maximum value and then decreases to zero, i.e. $\nu_\theta = 0$ for $a = M$, $r = M$. The ratio of the frequencies, ν_0/ν_θ , essentially differs from unity only for the fast enough rotation of the black hole. For the retrograde motion both frequencies decrease with the growth of the rotation parameter (see also Eq. (11)), whereas their ratio remains about unity.

It is also of interest to calculate all the three frequencies at direct stable orbits beyond ISCO ($r > r_{ISCO}$) around an extreme rotating black hole, $a = M$. The results of numerical calculations are presented in Table II. We observe that at particular orbits near the black hole, the predicted values of the epicyclic frequencies (bolded in the table) are close to the corresponding frequencies of twin peaks QPOs, which are in a 3:2 ratio and have been detected in some black hole binaries: For instance, to (184, 276 Hz) for X-ray binary XTE J1550-564; to (165, 241 Hz) for X-ray binary H1743-322; to (113, 168 Hz) for X-ray binary GRS 1915 + 105.

A. The highest epicyclic frequencies

It is interesting that there exist the highest epicyclic frequencies of small oscillations around circular orbits in the Kerr field. This fact was first noted in [39], for the frequency of radial oscillations given by expression (8). Evaluating the first derivative of this expression with respect to r , we obtain the equation

$$r^3(8M - r) + a^2(5r^2 - 4Mr) \pm 2a\sqrt{Mr}[a^2 + r(M - 6r)] = 0. \quad (12)$$

This equation determines the radii for both direct and retrograde orbits, at which the radial epicyclic frequency attains its highest value. For the Schwarzschild case, $a = 0$, it follows that $r_{max} = 8M$ and the associated frequency $\nu_{r(max)} \simeq 707.1 (M_\odot/M) \text{ Hz}$. Meanwhile, for $a \neq 0$, equation (12) can be solved only numerically. In particular, for $a = M$ and for the direct orbit, we find that $r_{max} \simeq 2.4M$ and

$$\nu_{r(max)} \simeq 2453 \left(\frac{M_\odot}{M} \right) \text{ Hz}. \quad (13)$$

Similarly, for the retrograde orbits at $a = M$, we have $r_{max} \simeq 11.8M$ and

$$\nu_{r(max)} \simeq 422.6 \left(\frac{M_\odot}{M} \right) \text{ Hz}. \quad (14)$$

In Figure 1 we plot the dependence of the radial epicyclic frequency on the radii of circular orbits around the Kerr black hole for different values of the rotation parameter and for $M = 10M_\odot$. The full numerical analysis of equation (12) and the associated values of

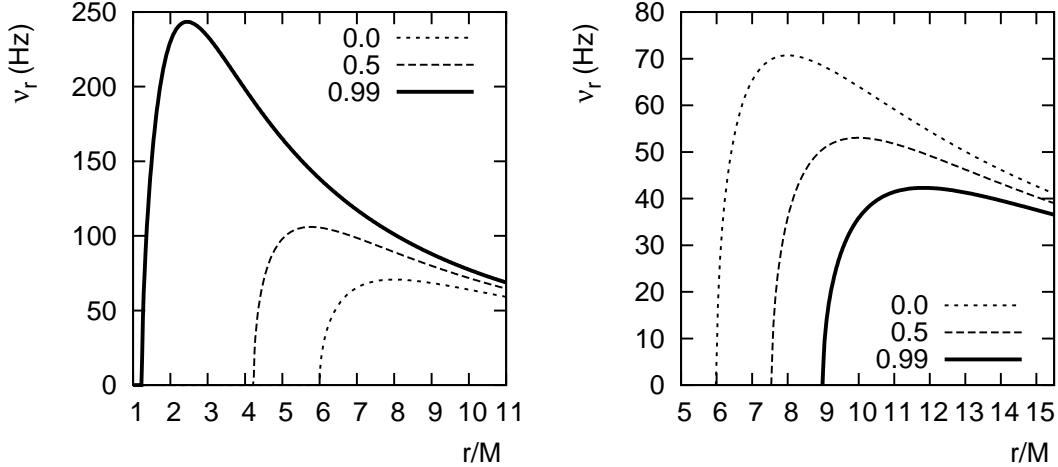


FIG. 1. Radial epicyclic frequencies with three values of the rotation parameter $a/M = 0, 0.5$ and 0.99 . (*Left*: For direct orbits. *Right*: For retrograde orbits).

the radial, vertical and orbital frequencies along with their corresponding ratios are given in Tables III and IV.

Comparing Figure 1 and Table III, we see that for the direct orbits, with increasing rotation parameter of the black hole, the maxima of the radial epicyclic frequency shifts towards the event horizon and in the limiting case $a = M$, the frequency attains its highest value in the near-horizon region. The accompanying vertical and orbital frequencies at the same radii also increase to their highest values for $a = M$. It is also interesting to note that the characteristic ratios $\nu_\theta : \nu_{r(max)} = 2 : 1$, $\nu_0 : \nu_{r(max)} = 2 : 1$ and $\nu_0 : \nu_\theta = 1 : 1$ remain almost unchanged up to large enough values of the rotation parameter. However, for $a \rightarrow M$ we have the approximate ratios $\nu_\theta : \nu_r = 9 : 5$, $\nu_0 : \nu_r = 5 : 2$ and $\nu_0 : \nu_\theta = 3 : 2$. *Thus, we conclude that at the characteristic stable circular orbits, where the radial epicyclic frequency attains its highest value, the ratio $\nu_\theta : \nu_r = 2 : 1$ remains nearly the same even for $a \rightarrow M$.* Remarkably, this fact is in good enough agreement with the observed twin QPOs frequencies in the X-ray spectrum of some black hole binaries. For instance, for $a \simeq (0.8-0.9)M$, the detected pair (164, 328 Hz) in the source GRS 1915 + 105 falls in the expected ranges of the radial ν_r and vertical ν_θ epicyclic frequencies given in Table III. Meanwhile, Figure 1 and Table IV for the retrograde orbits show that the highest value of the radial frequency

at $a = 0$ as well as the associated values of the vertical and orbital frequencies decrease with the growth of the rotation parameter and attain their characteristic values in the limiting case $a = M$. It is also interesting to note that the frequencies exhibit, to a good enough accuracy, the ratios $\nu_\theta : \nu_{r(max)} = 2 : 1$, $\nu_0 : \nu_{r(max)} = 2 : 1$ and $\nu_0 : \nu_\theta = 1 : 1$.

We turn now to the expression of the vertical epicyclic frequency given in (9). For direct orbits and for sufficiently large values of the rotation parameter, this frequency attains its highest value as well. The radii of characteristic orbits, pertaining to the maxima of the vertical frequency, are given by the equation

$$r \left[r^3 + a^2 (5r - 2M) \right] + 2a\sqrt{Mr} (a^2 - 3r^2) = 0. \quad (15)$$

Solving this equation numerically for $a = M$, we find that $r_{(max)} \simeq 1.86M$ and the highest vertical frequency is

$$\nu_{\theta(max)} \simeq 4875 \left(\frac{M_\odot}{M} \right) Hz, \quad (16)$$

whereas, the radial frequency at this radius has the value

$$\nu_r \simeq 2236 \left(\frac{M_\odot}{M} \right) Hz. \quad (17)$$

It is easy to see that the approximate ratio $\nu_{\theta(max)} : \nu_r = 2 : 1$ holds in this case as well.

In Figure 2 we plot the vertical epicyclic frequency as a function of the radius of direct orbits, for given values of the rotation parameter and for $M = 10M_\odot$ (*Left*). Here we also plot the positions of ISCOs and $\nu_{\theta(max)}$ as the functions of the rotation parameter (*Right*). We see that the vertical frequency reaches its highest value in the region of physical interest, $r_{(max)} > r_{ISCO}$.

III. GEODESIC MOTION AND EPICYCLIC FREQUENCIES AROUND ROTATING BRANEWORLD BLACK HOLES

The measurements of the angular momenta of black holes harbored in a number of X-ray binaries reveal high enough values, approaching in some cases the extreme Kerr limit. For instance, the *lower bound* on the rotation parameter of the black hole in the X-ray binary GRS 1915 + 105 turns out to be very close to the (*upper*) Kerr bound for rotating black holes in general relativity [30]. Although similar results are somewhat model-dependent, nevertheless they reinforce the belief that a black hole that possesses an angular momentum

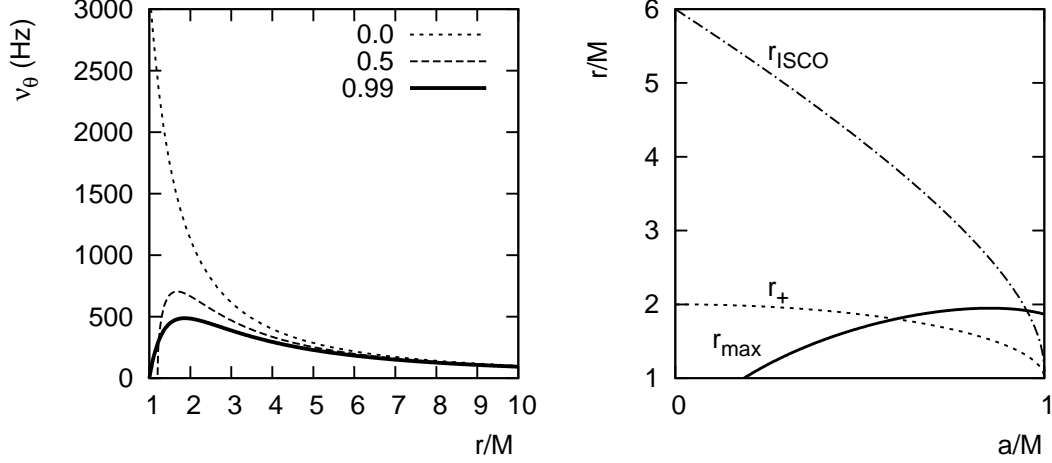


FIG. 2. Direct orbits: Vertical epicyclic frequencies with the rotation parameter $a/M = 0, 0.5$ and 0.99 (*Left*). Positions of ISCOs and $\nu_{\theta(max)}$ as the functions of the rotation parameter (*Right*).

greater than the Kerr bound could exist. This in turn stimulates the study of the observable effects of black holes with over-Kerr bound angular momenta (“over-rotating” black holes). In this section, we explore this possibility in an instructive model of geodesic motion around a rotating black hole localized on a 3-brane in the Randall-Sundrum scenario [20]. Such a black hole carries a tidal charge, as an imprint of the extra fifth dimension, and breaches the Kerr bound for the negative value of the tidal charge. The associated spacetime metric in Boyer-Lindquist coordinates is given by

$$ds^2 = -\frac{\Delta}{\Sigma} (dt - a \sin^2 \theta d\phi)^2 + \Sigma \left(\frac{dr^2}{\Delta} + d\theta^2 \right) + \frac{\sin^2 \theta}{\Sigma} [adt - (r^2 + a^2) d\phi]^2, \quad (18)$$

where

$$\Delta = r^2 + a^2 - 2Mr + \beta, \quad \Sigma = r^2 + a^2 \cos^2 \theta. \quad (19)$$

Here M and a are the mass and rotation parameters, respectively and the parameter β is the tidal charge. This metric is the reminiscent of the usual Kerr-Newman metric in which the electric charge of the black hole is superseded by the tidal charge. Solving the equation $\Delta = 0$, we find that the radius of the event horizon is given by

$$r_+ = M + \sqrt{M^2 - a^2 - \beta}, \quad (20)$$

which implies the relation

$$M^2 \geq a^2 + \beta, \quad (21)$$

where the equality holds in the extreme case. We see that *for the positive tidal charge, the angular momentum of the braneworld black hole does not exceeds its mass, whereas for the negative tidal charge it is greater than the mass.* The detailed analysis of the properties of metric (18) can be found in [20, 25].

The circular motion of test particles in metric (18) occurs in the equatorial plane $\theta = \pi/2$, whose orbital frequency Ω_0 has the same form as given in (5), where the Kepler frequency is now given by $\Omega_s = (Mr - \beta)^{1/2}/r^2$. As for the energy of the test particles, it can be found either by substituting in equation (4) the nonvanishing components of the Christoffel symbols and repeating all the steps leading to equation (6) or simply replacing the square of the electric charge by the tidal charge, in the corresponding expression for the usual Kerr-Newman metric (see, for instance [35]). As a result, we have

$$\frac{E}{m} = \frac{r^2 - 2Mr + \beta \pm a\sqrt{Mr - \beta}}{r \left[r^2 - 3Mr + 2\beta \pm 2a\sqrt{Mr - \beta} \right]^{1/2}}. \quad (22)$$

The vanishing denominator of this expression gives the radius of the limiting photon orbit. For $\beta = M^2$, the limiting radius is the same as for an extreme Reissner-Nördstrom black hole, $r_{ph} = M$ ($r_+ = M$). Meanwhile, for the negative tidal charge $\beta = -M^2$ ($a = \sqrt{2}M$, $r_+ = M$), the limiting radii are $r_{ph} = M$ for the the direct motion and $r_{ph} = 4.82M$ for the retrograde one [20].

As for the epicyclic motion, its frequency in the radial direction is given by

$$\Omega_r^2 = \frac{\Omega_0^2}{Mr - \beta} \left[Mr \left(1 - \frac{6M}{r} - \frac{3a^2}{r^2} + \frac{9\beta}{r^2} \right) + \frac{4\beta}{r^2} (a^2 - \beta) \pm 8a\Omega_s(Mr - \beta) \right], \quad (23)$$

while, for the frequency in the vertical direction we have

$$\Omega_\theta^2 = \Omega_0^2 \left[1 + \frac{a^2}{r^2} \left(1 + \frac{2Mr - \beta}{Mr - \beta} \right) \mp 2a\Omega_s \frac{2Mr - \beta}{Mr - \beta} \right]. \quad (24)$$

We note that these expressions were also given in [25] and they can be obtained from the general expressions for the Kerr-Newman field, earlier found in [35], in which one needs to change the square of the electric charge to the tidal charge, keeping in mind that the latter may have both positive and negative values. For the vanishing tidal charge, $\beta = 0$, these expressions go over into those given in (8) and (9). The boundaries of the ISCOs in the radial direction are governed by the equation $\Omega_r^2 = 0$. The analysis of this equation shows that for $\beta = M^2$, the limiting radius is $r_{ms} = 4M$ just as for an extreme Reissner-Nördstrom

black hole, whereas for an over-rotating black hole with $\beta = -M^2$ ($a = \sqrt{2}M$) we have $r_{ms} = M$ for the direct motion and $r_{ms} \simeq 11.25M$ for the retrograde one (see [20, 25] for details). Meanwhile, the analysis of expression (24) shows that the vertical motion is stable against linear perturbations in this direction.

It turns out that the radial epicyclic frequency in (23) has maxima at some characteristic orbits, just as expression (8) for the Kerr field. In what follows, we will focus on this case. Assuming first that the black hole has a small positive tidal charge, we compute all three fundamental frequencies and their corresponding ratios at direct orbits, for which the radial frequency in (23) attains its maximum value. The numerical results are summarized in Table V.

Comparing these results with those given in Table III, we see that the observed pair of frequencies (164, 328 Hz) in the source GRS 1915 + 105 falls in the range of the radial ν_r and vertical ν_θ frequencies that corresponds to less values of the rotation parameter, $a \simeq (0.7\text{--}0.8)M$. On the other hand, recent observations give the lower bound $a > 0.98M$ on the rotation parameter of the black hole in GRS 1915 + 105 [30]. Nevertheless, this discrepancy still might not be enough on its own to judge about the observational appearance (or non-appearance) of the positive tidal charge as the reported constraint on the bound of the rotation parameter is highly model-dependent. In some other cases, this constraint is found to be much below (see, for instance, [43, 44]). The reason for this is that the measurements of the rotation parameter of the black hole are obtained by modeling the thermal X-ray continuum of its accretion disk spectra to infer the inner radius of disk with subsequently identifying it with that of ISCO, which depends only on the mass and rotation parameter of the black hole. However, the accretion disk spectra are generally complex being accompanied by a radiative tail of non-thermal nature as well as by the imprints of relativistic effects. Depending on the model under consideration, these may have a large impact on the estimate of the rotation parameter.

Meanwhile, there exists a fundamental constraint on the values of the positive tidal charge and the rotation parameter, governed by equation (20), i.e. by the very existence of the black hole. It follows from this equation that with the growth of the positive tidal charge, the rotation parameter must decrease and for the large enough charge, $\beta \rightarrow M^2$, the rotation parameter tends to zero. Furthermore, performing the above numerical analysis of the epicyclic frequencies for the tidal charge $\beta = 0.99M^2$, which implies the highest rotation

parameter $a = 0.1M$, we find the pair of frequencies $(\nu_r, \nu_\theta) = (118, 249 \text{ Hz})$. This pair lies far enough away from the detected pair of frequencies $(164, 328 \text{ Hz})$ in the source GRS 1915 + 105. On the basis of all that has been said above, we can conclude that *at least, the large enough positive tidal charge is not supported by the observations of QPOs in black hole systems.*

Next, we suppose that the black hole possesses the negative tidal charge $\beta = -M^2$ and again calculate all three frequencies at the characteristic direct orbits, at which the radial epicyclic frequency attains its maxima. The results are given in Table VI. Comparing these results with those given in Table III, it is easy to see that the negative tidal charge has an enlarging effect on the radii r_{max} , whereas with increasing the rotation parameter of the black hole, the radii again move towards the event horizon, approaching the limiting value for $a = \sqrt{2}M$. We also see the appearance of the approximate 2 : 1 ratio between the vertical and radial epicyclic frequencies. It is important to note that in the over-rotating case, $a \simeq 1.27M$, the values of the radial ν_r and vertical ν_θ frequencies and their ratio are in good enough agreement with the detected pair of frequencies $(164, 328 \text{ Hz})$ in the source GRS 1915 + 105.

Figure 3 displays the positions of the maxima of the radial epicyclic frequencies for an extreme Kerr black hole and for an over-rotating braneworld black hole with the negative tidal charge $\beta = -M^2$. We see that the epicyclic frequencies in the field of these black holes are observationally almost indistinguishable. We note that it is the value of the angular momentum (for instance, reported from independent observations) that would play a crucial role to distinguish between these two black holes and the over-Kerr bound value of the angular momentum would be in favor of the potential existence of the braneworld black hole in the universe.

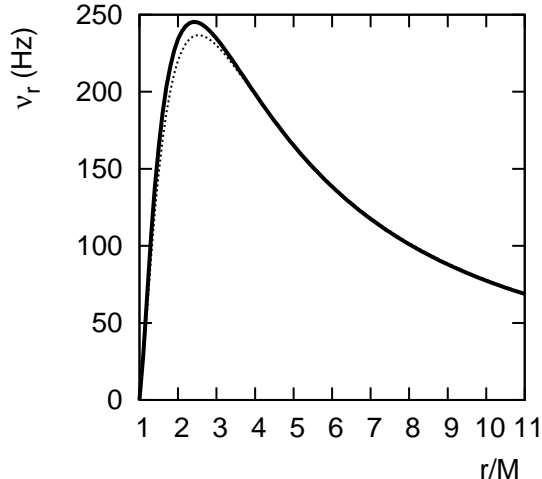


FIG. 3. The radial epicyclic frequencies for the direct orbits. The solid line corresponds to the extreme Kerr black hole, $\beta = 0$, $a = M$ and the dotted line refers to the braneworld black hole, $\beta = -M^2$, $a = \sqrt{2}M$.

IV. CONCLUSION

In general relativity, the circular motion of test particles around rotating black holes can be described in terms of three fundamental frequencies: The orbital (cyclic) frequency, the epicyclic frequency of radial oscillations and the epicyclic frequency of vertical oscillations [35–38]. All three of these frequencies are different, encapsulating somewhat the effects of strong gravity regime near the black holes. Remarkably, the epicyclic frequencies of radial and vertical oscillations can be related to the frequencies of twin peaks high-frequency QPOs, discovered in a number of black hole binaries. The purpose of this paper was to explore these issues in more detail from the general relativistic point of view. We have considered two instructive models of the geodesic motion; around a Kerr black hole in general relativity and around a rotating black hole in braneworld gravity. In both cases, we have performed a detailed numerical analysis of the fundamental frequencies at the stable orbits of interest and found the examples of observationally viable cases of the epicyclic frequencies.

As the main result for the Kerr black hole, we have found that for a class of stable orbits, where the radial (or the vertical) epicyclic frequency attains its maxima, the vertical and radial epicyclic frequencies are in an approximate 2 : 1 ratio, occurring even for near-extreme rotation of the black hole. We have also found that for the rotation parameter in the

range $a \simeq (0.8\text{--}0.9)M$, the values of the epicyclic frequencies underlying this ratio exhibit good enough qualitative agreement with the detected twin peaks frequencies of QPOs in the source GRS 1915 + 105 which, to our best knowledge, appears to be a unique case so far. Furthermore, we have found that at particular class of orbits near the black hole, the predicted values of the epicyclic frequencies (bolded in Table II) are close to the frequencies of twin peaks QPOs, which are in a 3:2 ratio and have been detected in some black hole binaries: For instance, to (184, 276 Hz) for X-ray binary XTE J1550-564; to (165, 241 Hz) for X-ray binary H1743-322; to (113, 168 Hz) for X-ray binary GRS 1915 + 105. These findings are substantially new. As we noted in the introduction, the idea of nonlinear resonances that may happen when the epicyclic frequencies are in a rational relation [35] has been utilized in the literature [33, 34] to develop the models for the observed high frequency QPOs. The results of our paper show that the simple model of pure geodesic motion can also provide, to some extent, the observationally viable values for the epicyclic frequencies, without invoking nonlinear resonances between them.

For the rotating braneworld with a tidal charge, we have performed the full numerical analysis of the epicyclic frequencies, focusing on the stable orbits, where the radial epicyclic frequency reaches its maximum value. Here we have found that while the large enough value of the positive tidal charge is not supported by the observations of high frequency QPOs, the situation is different for the negative tidal charge. For the large enough value of the negative tidal charge, the braneworld black hole exhibits close similarities with the Kerr black hole, including the appearance of the approximate 2 : 1 ratio between the vertical and radial epicyclic frequencies. We have also found that in the case under consideration, the over-rotating braneworld black hole and the extreme Kerr black hole are almost indistinguishable in the high-frequency QPOs observations. We note that these results are also substantially new. On these grounds, we concluded that the potential existence of the over-rotating braneworld black hole with the negative tidal charge does not confront with modern observations of the black hole systems in the universe.

V. ACKNOWLEDGMENTS

One of us (A. N. Aliev) thanks Ekrem alkılı for his invaluable support and encouragement. The work of G. D. E. is supported by Istanbul University Scientific Research Project (BAP) No. 3149.

- [1] Penrose R 1965 *Phys. Rev. Lett.* **14** 57; Hawking S W and Penrose R (1970) *Proc. Roy. Soc. Lond.* **A314** 529
- [2] Israel W 1967 *Phys. Rev.* **164** 1776; Carter B *Phys. Rev. Lett.* 1971 **26** 331
- [3] Hawking S W 1972 *Commun. Math. Phys.* **25** 152; Robinson D C 1975 *Phys. Rev. Lett.* **34** 905
- [4] Carter B 1968 *Phys. Rev. D* **174** 1559
- [5] Chandrasekhar S 1983 *The Mathematical Theory of Black Holes* (Clarendon Press, Oxford)
- [6] Frolov V P and Novikov I D 1998 *Physics of Black Holes* (Kluwer Academic Press, Dordrecht)
- [7] Kerr R P 1963 *Phys. Rev. Lett.* **11** 237
- [8] Bardeen J M, Press W H and Teukolsky S A 1972 *Astrophys. J.* **178** 347
- [9] Shapiro S L and Teukolsky S A 1983 *Black Holes, White Dwarfs and Neutron Stars* (A Wiley-Interscience Publ., New York)
- [10] Myers R C and Perry M J 1986 *Ann. Phys. (N.Y.)* **172** 304
- [11] Emparan R and Reall H S 2002 *Phys. Rev. Lett.* **88** 101101
- [12] Arkani-Hamed N, Dimopoulos S and Dvali G 1998 *Phys. Lett. B* **429**, 263; Antoniadis I, Arkani-Hamed N, Dimopoulos S and Dvali G 1998 *Phys. Lett. B* **436** 257
- [13] Randall L and Sundrum R 1999 *Phys. Rev. Lett.* **83** 3370; Randall L and Sundrum R 1999 *Phys. Rev. Lett.* **83** 4690
- [14] Giddings S B and Thomas S 2002 *Phys. Rev. D* **65** 056010
- [15] Gal'tsov D V, Kofinas G, Spirin P and Tomaras T N 2010 *Phys. Lett. B* **683** 331
- [16] Berti E, Kokkotas K D and Papantonopoulos E 2003 *Phys. Rev. D* **68** 064020
- [17] Chamblin A, Hawking S W and Reall H S 2000 *Phys. Rev. D* **61** 065007
- [18] Gregory R and Laflamme R 1993 *Phys. Rev. Lett.* **70** 2837
- [19] Dadhich N, Maartens R, Papadopoulos P and Rezanian V 2000 *Phys. Lett. B* **487** 1

- [20] Aliev A N and Gümrükçüoğlu A E 2005 *Phys. Rev. D* **71** 104027
- [21] Shiromizu T, Maeda K and Sasaki M 2000 *Phys. Rev. D* **62** 024012
- [22] Aliev A N and Gümrükçüoğlu A E 2004 *Class. Quant. Grav.* **21** 5081
- [23] Kotrlová A , Stuchlík Z and Török G 2008 *Class. Quant. Grav.* **25** 225016
- [24] Stuchlík Z and Kotrlová A 2009 *Gen. Relat. Gravit.* **41** 1305; Schee J and Stuchlík Z 2009 *Int. J. Mod. Phys. D* **18** 983
- [25] Aliev A N and Talazan P 2009 *Phys. Rev. D* **80** 044023
- [26] Bambi C 2012 *Phys. Rev. D* **85** 043002
- [27] Özel F, Psaltis D, Narayan R and McClintock J E 2010 *Astrophys. J.* **725** 1918
- [28] Remillard R A and McClintock J E 2006 *Ann. Rev. Astron. Astrophys.* **44** 49
- [29] L. Gou L, McClintock J E, Reid M J et al. 2011 *Astrophys. J.* **742** 85
- [30] McClintock J E, Shafee R, Narayan R et al. 2006 *Astrophys. J.* **652** 518
- [31] Gimon E G and Horava P 2009 *Phys. Lett. B* **672** 299
- [32] Stella L and Vietri M 1999 *Phys. Rev. Lett.* **82** 17
- [33] Abramowicz M A and Kluźniak W 2001 *Ast.& Ap.* **379** L19
- [34] Abramowicz M A and Kluźniak W 2004 *X-ray Timing 2003: Rossie and Beyond*, AIP Conference Proceedings **714** 21; astro-ph/0312396
- [35] Aliev A N and Gal'tsov D V 1981 *Gen. Relat. Gravit.* **13** 899
- [36] Aliev A N, Gal'tsov D V and Petukhov V I 1986 *Astr. Space Sci.* **124** 137
- [37] Aliev A N and Galt'sov D V 1988 *Sov. Astron. Lett.* **14**(1) 48
- [38] Aliev A N and Gal'tsov D V 1989 *Sov. Phys. Usp.* **32**(1) 75
- [39] Okazaki A, Kato S and Fukue J 1987 *Publ. Astron. Soc. Japan* **39** 457
- [40] Kato S 1990 *Publ. Astron. Soc. Japan* **42** 99
- [41] Frolov V P and Stojković D 2003 *Phys. Rev. D* **68** 064011
- [42] Aliev A N 2008 *Proceedings of the 11th Marcel Grossmann Meeting on General Relativity* p.1057, Berlin, Germany; astro-ph/0612730
- [43] Middleton M, Done C, Gierliński M and Davis S W 2006 *Mon. Notes Roy. Astron. Soc.* **373** 1004
- [44] Blum J L, Miller J M, Fabian A C et al. 2009 *Astrophys. J.* **706** 60

TABLE I. Orbital and vertical frequencies at ISCOs ($M = 10M_\odot$)

	direct orbits				retrograde orbits			
a/M	r_{ms}/M	$\nu_0(Hz)$	$\nu_\theta(Hz)$	ν_0/ν_θ	r_{ms}/M	$\nu_0(Hz)$	$\nu_\theta(Hz)$	ν_0/ν_θ
0.00	6.00	217.73	217.73	1.00	6.00	217.73	217.73	1.00
0.10	5.67	235.32	231.91	1.01	6.32	202.54	205.15	0.99
0.20	5.33	255.93	248.03	1.03	6.64	189.28	193.91	0.98
0.30	4.98	280.49	266.52	1.05	6.95	177.59	183.79	0.97
0.40	4.61	310.32	287.97	1.08	7.25	167.20	174.65	0.96
0.50	4.23	347.48	313.16	1.11	7.55	157.92	166.33	0.95
0.60	3.83	395.41	343.20	1.15	7.85	149.56	158.74	0.94
0.70	3.39	460.42	379.58	1.21	8.14	142.02	151.81	0.94
0.80	2.91	556.00	423.99	1.31	8.43	135.12	145.38	0.93
0.90	2.32	721.41	474.68	1.52	8.72	128.84	139.47	0.92
0.99	1.24	1348.05	304.86	4.42	8.99	123.19	134.10	0.92

 TABLE II. Frequencies at direct stable orbits ($r > r_{ISCO}$, $a = M = 10M_\odot$)

r/M	$\nu_r(Hz)$	$\nu_\theta(Hz)$	$\nu_0(Hz)$	ν_θ/ν_r	ν_0/ν_r	ν_0/ν_θ
2.00	234.08	484.35	835.85	2.07	3.57	1.73
2.30	244.60	462.27	712.99	1.89	2.91	1.54
2.90	237.48	398.45	538.85	1.68	2.27	1.35
3.50	217.25	337.58	423.96	1.55	1.95	1.26
3.80	206.12	311.02	380.61	1.51	1.85	1.22
4.10	195.14	287.13	344.02	1.47	1.76	1.20
4.30	188.05	272.60	322.69	1.45	1.72	1.18
4.60	177.86	252.71	294.50	1.42	1.66	1.17
4.90	168.28	234.89	270.12	1.40	1.61	1.15
5.00	165.23	229.37	262.72	1.39	1.59	1.15
5.30	156.49	213.94	242.40	1.37	1.55	1.13
5.60	148.36	200.05	224.53	1.35	1.51	1.12
5.90	140.81	187.51	208.73	1.33	1.48	1.11
6.20	133.80	176.17	194.67	1.32	1.45	1.11
6.50	127.30	165.87	182.11	1.30	1.43	1.10
6.80	121.27	156.50	170.83	1.29	1.41	1.09
7.00	117.48	150.71	163.93	1.28	1.40	1.09

TABLE III. The highest radial frequency and the associated vertical and orbital frequencies at direct orbits ($M = 10M_\odot$)

a/M	r_{max}/M	$\nu_r(\text{Hz})$	$\nu_\theta(\text{Hz})$	$\nu_0(\text{Hz})$	ν_θ/ν_r	ν_0/ν_r	ν_0/ν_θ
0.00	8.00	70.71	141.42	141.42	2.00	2.00	1.00
0.10	7.58	75.73	151.17	152.60	2.00	2.02	1.01
0.20	7.15	81.52	162.37	165.68	1.99	2.03	1.02
0.30	6.70	88.27	175.45	181.26	1.99	2.05	1.03
0.40	6.24	96.29	190.74	199.97	1.98	2.08	1.05
0.50	5.76	105.99	209.23	223.29	1.97	2.11	1.07
0.60	5.26	118.03	231.78	252.90	1.96	2.14	1.09
0.70	4.71	133.53	260.59	292.71	1.95	2.19	1.12
0.80	4.11	154.57	298.90	349.83	1.93	2.26	1.17
0.90	3.42	185.95	353.95	442.93	1.90	2.38	1.25
0.99	2.45	243.45	447.52	662.11	1.84	2.72	1.48
1.00	2.42	245.34	450.40	671.62	1.84	2.74	1.49

TABLE IV. The highest radial frequency and the associated vertical and orbital frequencies at retrograde orbits ($M = 10M_\odot$)

a/M	r_{max}/M	$\nu_r(\text{Hz})$	$\nu_\theta(\text{Hz})$	$\nu_0(\text{Hz})$	ν_θ/ν_r	ν_0/ν_r	ν_0/ν_θ
0.00	8.00	70.71	141.42	141.42	2.00	2.00	1.00
0.10	8.41	66.31	132.83	131.72	2.00	1.99	0.99
0.20	8.81	62.42	125.20	123.24	2.01	1.97	0.98
0.30	9.21	58.95	118.38	115.74	2.01	1.96	0.98
0.40	9.60	55.84	112.25	109.08	2.01	1.95	0.97
0.50	9.98	53.03	106.70	103.10	2.01	1.94	0.97
0.60	10.36	50.48	101.65	97.72	2.01	1.94	0.96
0.70	10.73	48.16	97.04	92.85	2.02	1.93	0.96
0.80	11.10	46.03	92.81	88.41	2.02	1.92	0.95
0.90	11.47	44.07	88.92	84.35	2.02	1.91	0.95
1.00	11.83	42.26	85.32	80.63	2.02	1.91	0.95

TABLE V. The highest radial frequency and the associated vertical and orbital frequencies for the positive tidal charge

direct orbits: $\beta = 0.1M^2$, $M = 10M_\odot$							
a/M	r_{max}/M	ν_r (Hz)	ν_θ (Hz)	ν_0 (Hz)	ν_θ/ν_r	ν_0/ν_r	ν_0/ν_θ
0.00	7.81	72.78	145.69	145.69	2.00	2.00	1.00
0.09	7.41	77.83	155.54	156.99	2.00	2.02	1.01
0.19	6.99	83.65	166.83	170.17	1.99	2.03	1.02
0.28	6.56	90.42	179.91	185.77	1.99	2.05	1.03
0.38	6.12	98.43	195.30	204.58	1.98	2.08	1.05
0.47	5.66	108.10	213.71	227.80	1.98	2.11	1.07
0.57	5.17	120.05	236.29	257.38	1.97	2.14	1.09
0.66	4.64	135.38	264.85	296.79	1.96	2.19	1.12
0.76	4.07	156.08	302.77	353.12	1.94	2.26	1.17
0.85	3.39	186.74	357.31	444.84	1.91	2.38	1.24
0.95	2.42	244.13	452.24	666.79	1.85	2.73	1.47

TABLE VI. The highest radial frequency and the associated vertical and orbital frequencies for the negative tidal charge

direct orbits: $\beta = -M^2$, $M = 10M_\odot$							
a/M	r_{max}/M	ν_r (Hz)	ν_θ (Hz)	ν_0 (Hz)	ν_θ/ν_r	ν_0/ν_r	ν_0/ν_θ
0.00	9.64	56.20	112.29	112.29	2.00	2.00	1.00
0.14	9.09	60.69	121.06	122.28	1.99	2.01	1.01
0.28	8.53	65.94	131.25	134.11	1.99	2.03	1.02
0.42	7.95	72.15	143.25	148.35	1.99	2.06	1.04
0.57	7.36	79.63	157.61	165.82	1.98	2.08	1.05
0.71	6.74	88.84	175.16	187.83	1.97	2.11	1.07
0.85	6.09	100.51	197.15	216.53	1.96	2.15	1.10
0.99	5.40	115.87	225.74	255.80	1.95	2.21	1.13
1.13	4.64	137.33	264.91	313.73	1.93	2.28	1.18
1.27	3.77	170.50	323.56	411.81	1.90	2.42	1.27
1.41	2.53	236.74	431.78	663.00	1.82	2.80	1.54